To cite this article: LI X, LI H X, HUANG Y. Design of connecting mechanism and motion response analysis on nuclear power platform [J/OL]. Chinese Journal of Ship Research, 2020, 15(1). http://www.ship-research.com/EN/Y2020/V15/I1/152.

DOI: 10.19693/j.issn.1673-3185. 01786

Design of connecting mechanism and motion response analysis on nuclear power platform

LI Xiang, LI Hongxia, HUANG Yi*

School of Naval Architecture Engineering, Dalian University of Technology, Dalian 116024, China

Abstract: [**Objectives**] To ensure marine nuclear reactor safety in deep-water ice regions, this paper proposes a design for an ice region nuclear power platform and spring damper connecting mechanism. [**Methods**] The platform and connecting mechanism simulation model is established using the three-dimensional potential theory and rigid-body dynamics. The spring and damper force is calculated, then connecting mechanism stiffness and damping coefficients are analyzed and the best scheme selected. The discrete element method is used to simulate ice load. The accuracy of the method is verified by calculating ice load on the experimental conical structure. Platform motion response is calculated under environmental loads of combined wave, wind and current, or ice, wind and current. [**Results**] The ice region load-bearing platform can resist ice load. The nuclear reactor supporting platform can resist a Fukushima nuclear accident maximum tsunami wave height and level 17 super typhoon combination under the action of the connecting mechanism and mooring system. Under the 10 000-year return-time storm action in the North Sea, the ratio of horizontal displacement to water depth, heave and pitch response and vertical acceleration of the nuclear reactor supporting platform are all smaller than those of an offshore floating nuclear plant (OFNP). [**Conclusions**] This design for a nuclear power platform and connecting mechanism can ensure nuclear reactor safety and stability in deep-water ice regions.

Key words: nuclear power platform; connecting mechanism; ice load; vibration reduction; motion response; mooring

CLC number: U663.7

0 Introduction

As global warming accelerates the melting of arctic sea-ice, regular navigable waters have emerged in the summer. In the context of economic globalization and deepening regional integration, the value of the North Pole in strategic, economic, scientific research, environmental protection, shipping routes, and resources has been rising. The development and utilization of arctic shipping routes and resources can have a huge impact on China's energy strategy and economic development. As the foundation for the polar region development and the important engineering equipment for energy supply, the nuclear power platform in the ice region can provide sufficient and stable energy [1]. Although nuclear energy may have potential safety risks, it is one of the most economical and environmentally friendly available energy sources with an unreplacable role [2]. Therefore, it is of great significance to improving the safety and reliability of nuclear power platforms. The application prospect of nuclear power platform is broad, and its related problems have become the hot spot of research in the world. Therefore, it is of great significance to carry out technical reserves.

At present, four types, including barge, gravity basic structure, sunken structure, and cylindrical structure, have been put forward for the offshore nuclear

Received: 2019 - 09 - 27 **Accepted:** 2020 - 01 - 08

Supported by: National Natural Science Foundation of China (51779042); National Key R & D Program of China (2017YFE0111400); Fundamental Research Funds for the Central Universities (DUT2019TD35)

Authors: LI Xiang, female, born in 1994, master degree candidate. Research interests: nuclear power platform in ice regions. E-mail: leexiang113@mail.dlut.edu.cn

LI Hongxia, female, born in 1980, Ph.D., associate professor. Research interests: dynamics of ships and marine structures. E-mail: li_hx@dlut.edu.cn

***Corresponding author:** LI Hongxia

power platform. The first two are applied to the shallow water near the shore, and the second two are applicable to the water depth of 100 m. In this regard, Russia has already taken the lead in the world. In 2007, the construction of its barge-type nuclear power station "Lomonosov" began, which is the world's first offshore nuclear power station. It is expected to start supplying power to the Russian Far East at the end of 2019. South Korea has developed a nuclear power plant of gravity basic structural type, and France has developed a nuclear power plant of Flexblue sunken type [3]. Massachusetts Institute of Technology (MIT) proposed the concept of offshore floating nuclear power platform (OFNP), which is fixed on the shore by mooring devices to avoid the impact of earthquakes and tsunamis [4], and its safety in the corresponding marine environment has also been evaluated [5]. However, none of the above contents has made an in-depth study of the nuclear power platforms in a deep-water ice region.

This paper will design the hull lines, general arrangement, and the mooring system of a nuclear power platform [6] with internal and external separation that can be used in deep-sea ice regions. The influence law of the change of the stiffness coefficient and damping coefficient of the connecting mechanism between the internal and external platforms on the motion response of the platform is emphatically studied. Then the optimal scheme is selected accordingly to weaken the impact of the motion of the environmental bearing platform on the nuclear reactor support platform.

1 Fundamental theory

Based on the three-dimensional potential theory and the rigid body dynamics, a theoretical prediction method for the motion response of the nuclear power platform in the ice region and spring damper connecting mechanism under complex environmental loads is established. The equation of the six-degree-of-freedom motion of the nuclear reactor support platform is as follows.

$$(\boldsymbol{M}_1+\delta\boldsymbol{M}_1)\ddot{X}_1+\boldsymbol{F}_{c1}\left(\dot{X}_1,t\right)+(\boldsymbol{K}_1+\boldsymbol{K}_{\mathrm{TL}})X_1=\boldsymbol{F}_1+\boldsymbol{F}_{k1}+\boldsymbol{F}_{c1} \quad (1)$$

The equation of the six-degree-of-freedom motion of the environmental bearing platform is as follows.

$$(\boldsymbol{M}_2+\delta\boldsymbol{M}_2)\ddot{X}_2+\boldsymbol{F}_{c2}\left(\dot{X}_2,t\right)+\boldsymbol{K}_2X_2+\boldsymbol{F}_{\mathrm{MOOR}}=\boldsymbol{F}_2+\boldsymbol{F}_{k2}+\boldsymbol{F}_{c2} \quad (2)$$

where the subscripts 1 and 2 represent the internal and external platforms respectively; $\boldsymbol{M}$ and $\delta\boldsymbol{M}$ are the mass and additional mass matrixes of the platform respectively; $\boldsymbol{F}c(\dot{X},t)$ is the damping coefficient matrix; $\boldsymbol{K}$ is the static water restoring stiffness matrix; $\boldsymbol{K}_{\mathrm{TL}}$ is the tension leg mooring stiffness matrix of the internal platform, $\boldsymbol{K}_{\mathrm{TL}}$=diag (0, 0, k_{TL3}, k_{TL4}, k_{TL5}, 0), which only provides three-degree-of-freedom stiffness outside the horizontal plane (heave, roll, and pitch); $\boldsymbol{F}_{\mathrm{MOOR}}$ is the mooring force of the external platform system, $\boldsymbol{F}_{\mathrm{MOOR}} = (f_1(X_2, t), f_2(X_2, t), f_3(X_2, t), f_4(X_2, t), f_5(X_2, t), f_6(X_2, t))^{\mathrm{T}}$. With the multi-point mooring method and the concentrated mass method, the mooring force of the composite cable at each degree of freedom can be calculated; $X, \dot{X}, \ddot{X}$ are the six-degree-of-freedom displacement, velocity, and acceleration of the two platforms respectively; $\boldsymbol{F}$ is the environmental load force, including the wave incident force and diffraction force, wind force, current force, and ice force, and the masking effect of external platform on the internal platform is considered here; $\boldsymbol{F}_k=(f_{k1}, f_{k2}, f_{k3}, 0, 0, 0)^{\mathrm{T}}$ and $\boldsymbol{F}_c=(f_{c1}, f_{c2}, f_{c3}, 0, 0, 0)^{\mathrm{T}}$, are the spring force and damping force of three degrees of freedom (surge, sway, and heave) of the two platforms respectively, and the influence of spring damping force on the motion response of degrees of freedom (roll, pitch, and yaw) is ignored here. The constraint on the nuclear power platform is the limitation of nuclear reactor acceleration. The acceleration limit of the floating nuclear reactor is broader than that of the land-based nuclear reactor. With the reference to Westinghouse SMR, the acceleration limit of the nuclear reactor is 0.25 g [3], which is even more stringent.

2 Scheme design

2.1 Design of nuclear power platform

The separated nuclear power platform in the ice region is composed of a nuclear reactor support platform and an environmental bearing platform. The environmental bearing platform is designed as an hourglass structure, and the lower-cone bevel can well resist the ice load. When a large ice field moves, the ice around the platform climbs upward and breaks during the climb, which has a good ice-breaking effect. The upper design can effectively increase the deck area to meet the use requirements. During the ice period, the phenomenon of sea ice climbing can be effectively reduced. During the ice-free period, the green water phenomenon can be reduced. The nuclear reactor support platform floats on the sea, which acts as a natural giant radiator and a shield against radiation. Nuclear reactors are designed below the waterline to be quickly flooded in the event of an emergency, which can minimize the damage.

The general layout of the platform adopts the modular assembly method, and the annular partitioned compartments are shown in Fig. 1. The main functional areas include a nuclear reaction area, a boiler area, a turbine area, a safe house, a spent fuel pool, a central control room, a security room, a living area, a maintenance hall, a storage area, an apron, etc. Users can replace modules regularly according to their needs, so as to ensure the continuous supply of energy and the recycling of modules.

The nuclear power platform operates in an ice region with a water depth of 1 000 m. The internal platform is moored with tension legs, which mainly limits the movement of three degrees of freedom (heave, roll, and pitch) outside the horizontal plane. By the four tension legs installed symmetrically at bottom of the platform, the buoyancy of the platform would be much greater than its own gravity, which would make the motion outside the platform's horizontal plane small and close to rigid. The external platform adopts a semi-tensioned four-point mooring system, which restricts the motion of three degrees of freedom (surge, sway, and yaw) in the horizontal plane. Four groups of 12 three-segment composite cables are selected for semi-tensioned mooring, with an angle of 90° between the groups and an angle of 5° between the cables. The chock is located at the lower edge of the platform, with a mooring radius of 1 850 m, a pre-tension of 1 980 kN, and a pre-tension dip angle of 42.9°. The specific mooring cable parameters are shown in Table 1. In the table, E is the elastic modulus of the material, and A is the cross-sectional area of the mooring cable.

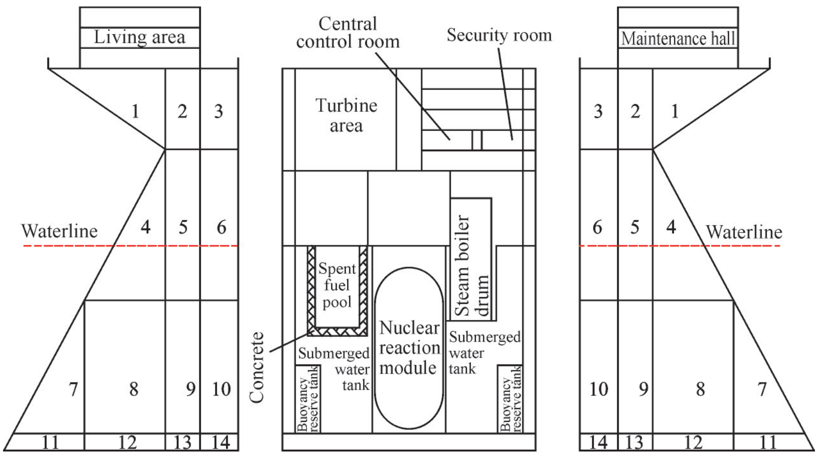

Fig.1 General layout of nuclear power platform in the ice region

Table 1 Parameters of mooring cable

Ingredient	Diameter/mm	Dry weight/(kg·m^{-1})	Breaking load/kN	EA/kN	Length/m
R4s Chain (High sea bottom)	84	131.32	7 989	620 340	140
Polyester (Middle section)	160	56.20	8 140	235 200	1 500
R4s Chain (Offshore bottom)	84	131.32	7 989	620 340	480

2.2 Design of connecting mechanism

The connecting mechanism is designed as four groups of springs and dampers, which are symmetrically installed in the middle of internal and external platforms (Fig. 2). The spring length is designed to be 7 m; the material is stainless steel wire used for spring; the shear modulus is 73×10^3 MPa; The elastic modulus is 195×10^3 MPa; the operating temperature is −200–+290 ℃. The material has strong properties and a wide temperature range, and the spring designed by this material can satisfy a wide range of stiffness. Both ends of the spring are fixed to the internal and external platforms by washers. There are guide holes at both ends of the washers, into which the spring can be put to maintain stability. The two ends of the damper are hinged with the main structure of the internal and external platform through the welding support of the steel structure. The connecting mechanism mainly limits the motion of the internal platform at the degrees of freedom of surge, sway, and heave but has little effect on other degrees of freedom.

Four groups of springs are connected to the internal and external platforms, and the equivalent stiffness and spring force of platforms are deduced according to the principle of equal deformation energy

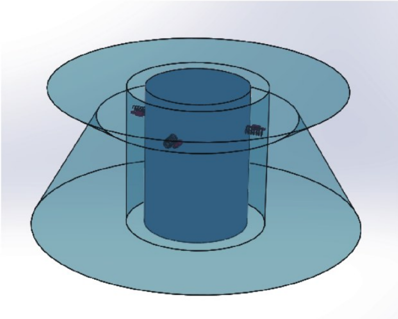

(a) Position diagram of connecting mechanism in platform

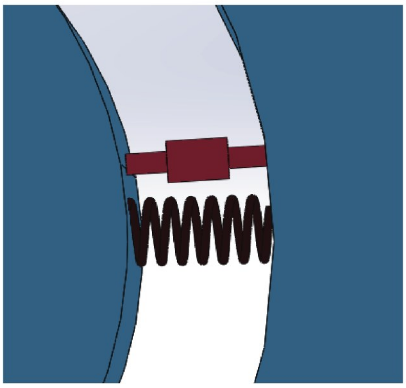

(b) Detail diagram of connecting mechanism

Fig.2 Schematic diagram of connecting mechanism

of the elastic elements. It is assumed that the original length of each spring is l_0; the stiffness is k; the relative displacement of internal and external platforms is l; the displacement projected to X, Y, and Z axes is respectively x, y, and z. Then spring deformation energy in the surge degree of freedom is $U_X = \sum_{i=1}^{4} U_{X_i} = U_{X_1} + U_{X_3} = kx^2 = 1/2k_X x^2$, so the equivalent stiffness in the surge degree of freedom is $k_X = 2k$. In the same way, the spring deformation energy of sway and heave degrees of freedom can be calculated as $U_Y = \sum_{i=1}^{4} U_{Y_i} = U_{Y_2} + U_{Y_4} = ky^2 = 1/2k_Y y^2$. and $U_Z = \sum_{i=1}^{4} U_{Z_i} = U_{Z_1} + U_{Z_2} + U_{Z_3} + U_{Z_4} = 2kz^2 = 1/2k_Z z^2$, and the equivalent stiffness of sway and heave degrees of freedom is k_Y=2k and k_Z=4k. Then the spring forces of surge and sway of internal platform and the spring force of heave of the external platform can be expressed as follows:

$$f_{k11} = -k_X x = -2kx \tag{3}$$

$$f_{k12} = -k_Y y = -2ky \tag{4}$$

$$f_{k23} = k_Z z = 4kz \tag{5}$$

The calculation of damping force is similar to that of spring force, so it is not repeated here.

As an important part of the nuclear power platform in the ice region, the connecting mechanism plays a role in vibration reduction, and its parameters have a great influence on the motion response of the nuclear reactor support platform. Considering the wave incident at 45° (see the wave parameters in Table 2 for once-in-ten-thousand-year sea condition), the influence of the damping coefficient c of the damper of the connecting mechanism and the stiffness coefficient k of the spring on the combined displacement with significant values of surge and sway of the internal platform is studied, and characteristics of the connecting mechanism are measured accordingly. The simulation results are shown in Fig. 3, and the corresponding cloud image is shown in Fig. 4.

Table 2 List of sea conditions for calculation

Level of sea condition	Significant wave height /m	Spectrum peak period /s	Average wind speed /(m·s^{-1})	Flow rate /(m·s^{-1})
Level 4	1.88	8.8	8.88	0.50
Level 5	3.25	9.7	11.45	0.50
Level 6	5.00	12.4	17.53	0.50
Extreme sea condition	23.00	19.3	70.00	2.76
Once-in-ten-thousand-year[5]	16.84	17.7	39.82	0.96

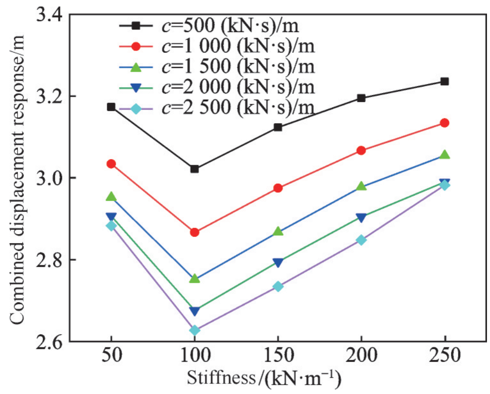

Fig.3 Effect of damping and stiffness coefficients on combined displacement

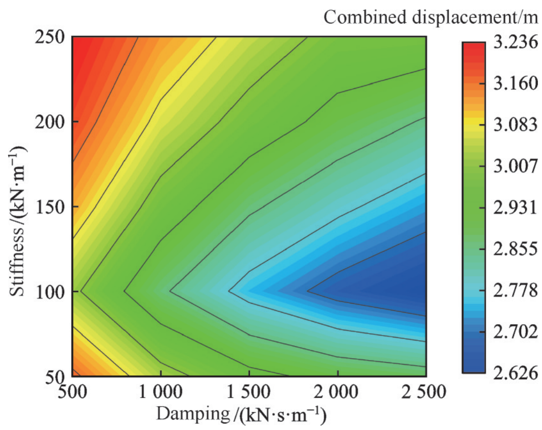

Fig.4 Effect contours of damping and stiffness coefficients on combined displacement

The combined displacement of the internal platform decreases gradually with the rise of the damping coefficient, and the decrease is more and more slow. This is because the increase in damping will reduce the dynamic amplification coefficient, thus limiting the motion response of the platform. The combined displacement decreases first and then increases with the rise in the stiffness coefficient. This is because the increase in stiffness reduces the static displacement, which further limits the motion response of the platform. After reaching a certain value, the natural frequency of the nuclear power platform is close to the concentrated energy frequency of the external wave load, which generates resonance, so the response of the platform increases.

Now, the damping coefficient c =2 000 (kN·s)/m is taken to calculate the natural frequency of the nuclear power platform when the stiffness coefficient is k = 25–250 kN/m. Considering only the surge degree of freedom, without considering the influence of damping and external force, the internal and external platforms constitute a two-degree-of-freedom system. The vibration equation can be expressed as follows.

$$\begin{bmatrix} m_1+\delta m_1 & 0 \\ 0 & m_2+\delta m_2 \end{bmatrix}\begin{bmatrix} \ddot{x}_1 \\ \ddot{x}_2 \end{bmatrix}+\begin{bmatrix} k_1 & -k_1 \\ -k_1 & k_1+k_2 \end{bmatrix}\begin{bmatrix} x_1 \\ x_2 \end{bmatrix}=\begin{bmatrix} 0 \\ 0 \end{bmatrix} \quad (6)$$

where m and δm are the mass and additional mass in the surge degree of freedom of two platforms; k_1 is the equivalent spring stiffness in the surge degree of freedom; k_2 is the stiffness in the surge degree of freedom of the mooring system; x and $\ddot{x}$ are respectively the displacement and acceleration of two platforms in the surge degree of freedom. The first-order and second-order frequencies are obtained as shown in Table 3. Due to the symmetry of the platform, the natural frequency in the sway degree of freedom is consistent with that of the surge. The wave force spectrum of the nuclear power platform is analyzed, and the frequency range of energy concentration is 0.34–0.56 rad/s. According to data in the table, when the stiffness is greater than 100 kN/m, the second-order frequency of the nuclear power platform is close to the concentrated frequency of wave force energy, and the response amplitude increases.

Considering the influence of the damping and stiffness coefficient on the internal platform comprehensively, the damping coefficient of the damper of the connecting mechanism is selected to be 2 000 (kN·s)/m and the spring stiffness coefficient is 100 kN/m based on the engineering practice experience. The vibration damping effect of this scheme is quite good, and the vibration mode is $\boldsymbol{\Phi}_1=\begin{bmatrix} 1 \\ 0.94 \end{bmatrix}$, $\boldsymbol{\Phi}_2=\begin{bmatrix} 1 \\ -0.27 \end{bmatrix}$.

Table 3 Effect of stiffness coefficient on platform frequency

Stiffness /(kN·m^{-1})	Combined displacement response/m	First-order frequency /(rad·s^{-1})	Second-order frequency /(rad·s^{-1})
25	2.98	0.061 9	0.147 8
50	2.91	0.062 9	0.205 7
75	2.72	0.063 2	0.250 8
100	2.68	0.063 3	0.288 9
125	2.72	0.063 4	0.322 6
150	2.79	0.063 5	0.353 1
200	2.90	0.063 6	0.407 2
250	2.98	0.063 7	0.455 0

Considering the coupling motion of all degrees of freedom of the nuclear power platform, the degrees of freedom (surge, sway, heave, roll, pitch, and yaw) of the platform supported by the nuclear reactor are respectively the first six degrees of freedom, and each degree of freedom of the environmental bearing platform is the last six degrees of freedom, which constitute a twelve-degree-of-freedom system. The natural frequency of the system and the corresponding mode are shown in Fig. 5.

Due to the symmetry of the system, it is easy to know that the natural frequencies and modes of roll and pitch, surge, and sway are the same. By analyzing the natural frequency and mode, we can be found that the first-order and second-order vibration modes are characterized by the coupling of surge and sway of the external and internal platforms, and the motion directions are the same. The first-order and second-order frequencies are the first-order natural frequency of surge and sway degrees of freedom, respectively. The fourth-order and fifth-order vibration modes are characterized by the coupling of surge and sway of the internal and external platforms, and the motion directions are opposite. The fourth-order and fifth-order frequencies are the second-order natural frequency of surge and sway degrees of freedom, respectively. The third-order vibration mode is characterized by yaw motion of the external platform and is relatively weakly coupled with other degrees of freedom. The third-order frequency is the first-order natural frequency in the yaw degree of freedom. The sixth-order vibration mode is characterized by yaw of the internal platform, and is extremely weakly coupled with other degrees of freedom. The sixth-order frequency is the second-order

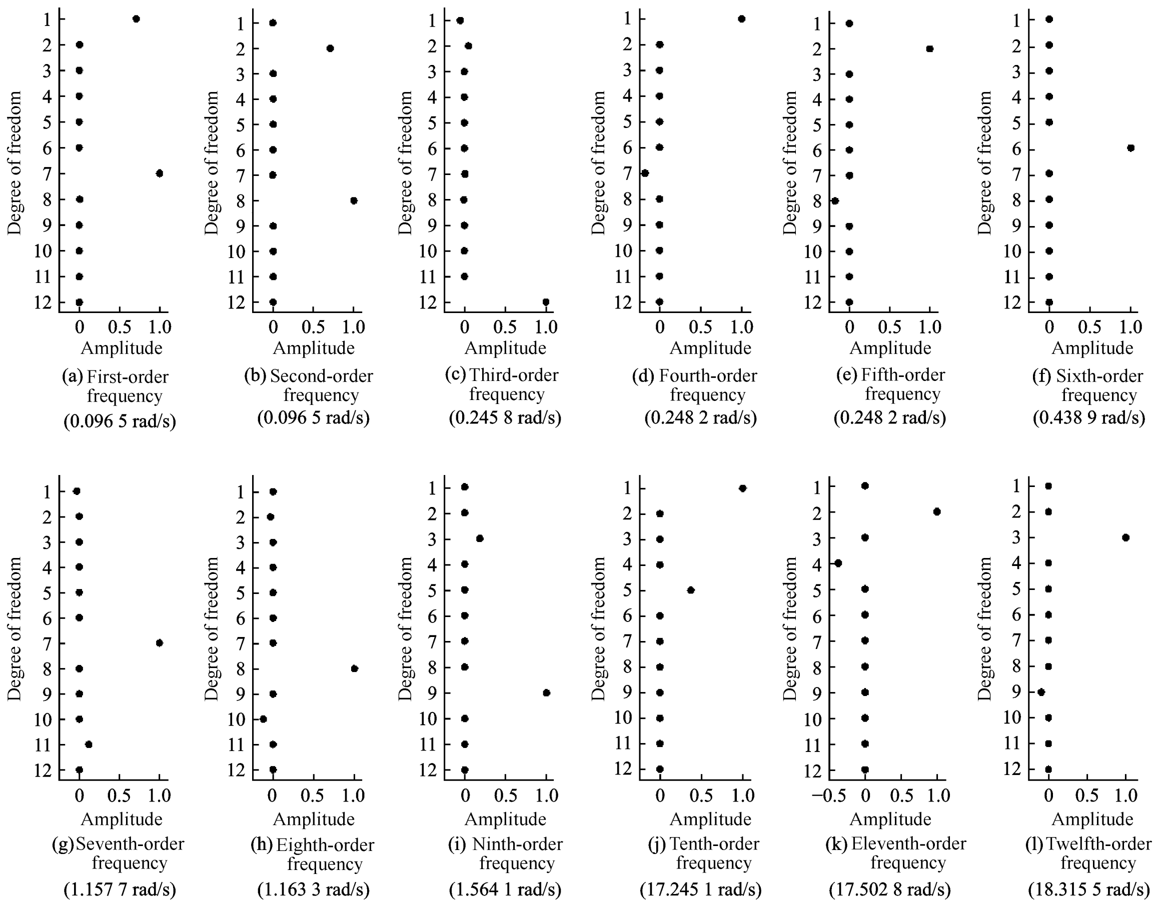

Fig.5 Natural frequency and vibration mode of nuclear power platform

natural frequency in the yaw degree of freedom. The seventh-order and eighth-order vibration modes are characterized by the coupling of surge and pitch as well as that of sway and roll of the external platform. The seventh-order and eighth-order frequencies are respectively the first-order natural frequency of the coupling of surge and pitch and that of sway and roll. The tenth-order and eleventh-order vibration modes are characterized by the coupling of surge and pitch and that of sway and roll of the internal platform. The tenth-order and eleventh-order frequencies are respectively the second-order natural frequency of the coupling of surge and pitch and that of sway and roll. The ninth-order vibration mode is characterized by the coupling of heave of the external and internal platforms, and the direction of motion is the same. The ninth-order frequency is the first-order natural frequency of the heave degree of freedom. The twelfth-order vibration mode is characterized by the coupling of heave of the internal and external platforms, and the direction of motion is the opposite. The twelfth-order frequency is the second-order natural frequency of the heave degree of freedom.

Considering that the natural frequency of surge obtained under the coupling of 12 degrees of freedom is close to that obtained by only considering the surge degree of freedom in Table 2, but due to more comprehensive considerations, it is closer to the actual situation. The response amplitude operator (RAO) for each degree of freedom corresponding to the 45° wave direction of the nuclear power platform is shown in Fig. 6.

The peak value of yaw RAO on the internal and external platforms is slightly less than 0.245 8 rad/s of the first-order natural frequency of yaw, which is caused by system damping and the result is reasonable. Heave RAO of the external platform has a very narrow peak RAO bandwidth (about 1.5) around 0.3 rad/s. On the two sides of RAO, however, there is a sharp decline. On the side with a lower frequency, the heave response is relatively stable. On the side with higher frequency, heave RAO increases rapidly from the minimum value to the second peak value (about 0.2) and then decreases slowly. The external platform is an hourglass floating body, and the natural period of heave is designed to be far away from the peak area of wave energy, so the platform has a relatively good performance of heave. The peak value of roll and pitch RAO of the internal and external platforms is located near 0.2 rad/s, which is slightly smaller than the second-order natural frequency of surge and sway, which is 0.248 rad/s. The second

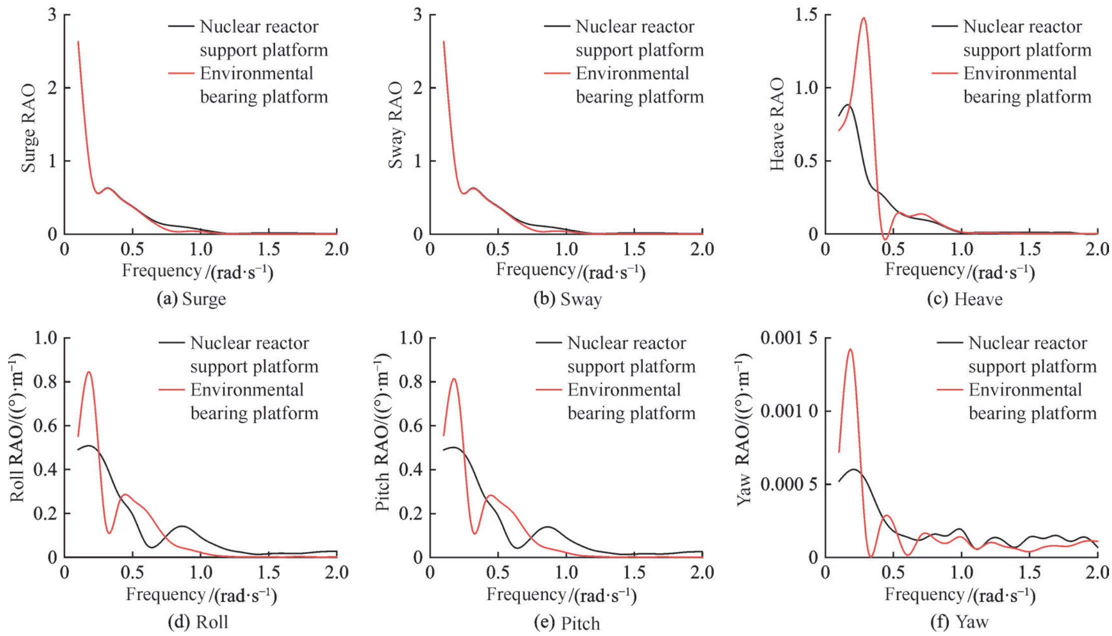

Fig.6 RAOs of nuclear power platform

peak of roll and pitch RAO of the internal and external platforms is located near 0.9 and 0.4 rad/s respectively, which is close to the first-order energy concentration frequency of the wave, requiring special attention.

3 Motion response

The nuclear power platform in the ice region is moored at a depth of 1 000 m in the Arctic Ocean, which can avoid the impact of tsunami, but the effect of wind, wave, current, ice, and other environmental loads should be considered. According to the data of wind speed and wave height in the Arctic Pole, we select the sea conditions of levels 4–6 for calculation by comparing with the sea condition table. Considering the extreme situation, the significant wave height is determined by reference to the maximum tsunami wave height of the Fukushima nuclear leakage accident (23 m). The wind load is selected by reference to OFNP calculation, which is a level 17 super typhoon. Other data are based on once-in-a-thousand-year sea condition in the South China Sea.

OFNP can withstand 10 000-year return-time storm in North Sea [5]. The same environmental conditions are selected, as shown in Table 2. Wind and current loads are considered as steady load, and the random wave load is simulated by JONSWAP spectrum. The ice load is simulated by the discrete element method, and the simulation model is established by means of the arrangement mode of the hexagonal close-packed structure [7]. The environmental load acts along the direction of 0°, 45°, and 90°. The nuclear power platform in the ice region is divided into two conditions, the ice-free period and the ice period. The corresponding environmental loads are the combined effect of wave, wind, and current with ice, wind, and current, respectively.

Table 4 Maximum motion response for combined action of wave, wind, and current

Degree of freedom	Nuclear reactor support platform					Environmental bearing platform				
	Level 4	Level 6	Extreme sea condition			Level 4	Level 6	Extreme sea condition		
	0°	0°	0°	45°	90°	0°	0°	0°	45°	90°
Surge/m	0.897	2.671	10.315	8.640	0.197	1.037	3.726	10.795	8.955	0.203
Sway/m	0.134	0.149	0.140	7.770	11.185	0.188	0.196	0.153	8.235	11.845
Heave/m	0.001	0.003	0.049	0.054	0.054	0.227	0.615	6.054	8.834	8.838
Roll /(°)	0.004	0.004	0.012	0.117	0.155	0.561	0.588	2.050	7.247	9.460
Pitch /(°)	0.007	0.027	0.129	0.112	0.001	0.542	1.907	8.354	5.860	0.868
Yaw /(°)	0.003	0.003	0.027	0.143	0.028	0.013	0.014	0.039	0.296	0.118

3.1 Combined effect of wave, wind, and current

The data in Table 4 give the maximum response result of the combined effect of wave, wind and current when the maximum wind and current are combined, namely, the wind direction is 90° and the flow direction is 90°. The wave direction is shown in Table 4, where surge, sway, and heave are the steady-state motion amplitude.

As can be seen from Table 4, surge, sway, and heave responses of the internal platform are relatively small, indicating that the connecting mechanism has achieved the expected function. In the extreme sea condition, the six-degree-of-freedom response of the internal platform is still small, revealing that the design of the connecting mechanism and the mooring system enables it to withstand the severe wave height and wind speed encountered in the Fukushima nuclear leakage accident, thus ensuring the safety of nuclear reactor. Under the action of level 17 super typhoon, OFNP can ensure that roll and pitch response is less than 5°; the vertical acceleration is less than $0.1g$ [4]; the maximum response value of roll and pitch of the nuclear reactor support platform is 0.155° and 0.129° respectively; the maximum vertical acceleration is 0.028 m/s^2(0.003g). It shows that its performance is better.

OFNP can withstand a 10 000-year return-time storm in North Sea [5]. Table 5 shows the maximum response under the combined effect of wave direction of 0°, 45°, 90°, wind direction of 90°, and flow direction of 90° subjected to the same environmental load. It can be seen from the table that the ratio of horizontal displacement to the water depth of the nuclear reactor support platform, heave and pitch responses, and vertical acceleration are all less than those of OFNP.

Table 5 Maximum motion response for extremely rare storm

Platform	Ratio of horizontal displacement to water depth/%	Heave/m	Pitch/(°)	Vertical acceleration /(m·s^{-2})
OFNP [5]	9.25	10.14	8.40	0.75
Nuclear reactor support platform	0.89	0.04	0.11	0.02
Environmental bearing platform	1.12	7.47	6.56	0.68

Considering that the nuclear reactor support platform rotates and the linear acceleration values at different points are varied, the acceleration of reactor cabin at the furthest point from the center of gravity of the platform is taken as the evaluation basis. The maximum acceleration at this point is calculated to be $0.029g$ at level 4, $0.053g$ at Level 6, and $0.193g$, $0.154g$, and $0.158g$ in the wave directions of 0°, 45°, and 90°, respectively, which satisfies the acceleration limitation of the land-based nuclear reactor. Fig. 7 shows the time history of nuclear reactor acceleration when the ultimate sea condition is 0° wave direction. Considering comprehensively, the nuclear power platform in the ice region can guarantee the nuclear reactor safety under the combined effect of wave, wind, and current.

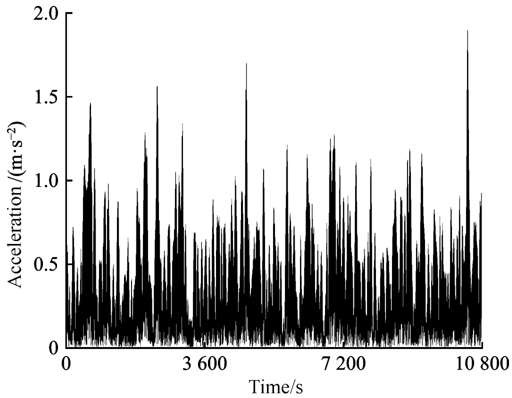

Fig.7 Acceleration time trace of nuclear reactor

3.2 Ice load calculation

The structural ice coating will have a great impact on the overall stability, structural integrity, moon pool, and so on [8], so the research on ice load is particularly important. IceDem software jointly developed by Dalian University of Technology and American Bureau of Shipping (ABS) is used for ice load simulation. It can simulate the contact forms of ships and marine structures with flat ice, crushed ice, pressure ridge, and other types, which can provide reference for the design of the ice resistant structure. Vertebral structure is a common design form of ice region structures, and the ice breaking effect is good. Therefore, the experimental data of vertebral structure is the preferred choice to verify the accuracy of numerical program. In this paper, a series of test data of Irani on hexahedral vertebra [9] are selected, and the scale ratio of test model is 1∶50, as shown in Fig. 8. The internal connecting diameter at the waterline of six-sided vertebral body is 30 m. The slope of each side is 5∶6, and the internal connecting diameter of the upper vertical structure is 10 m. In order to prevent the accumulation of crushed ice, we set a transition zone with a slope of 2∶1 on each side between the main structure and the upright structure of the vertebral body.

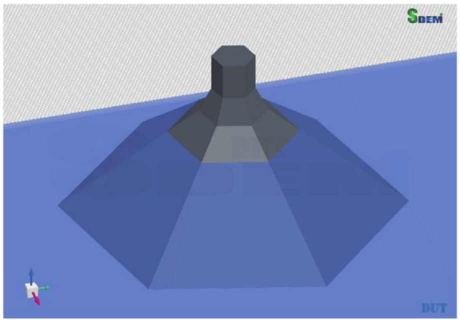

Fig.8 Numerical simulation model of hexahedral vertebral

In order to verify the accuracy of the simulation program, qualitatively, we make a comparison between the experimental conditions of C_006 and the time history of ice force obtained by numerical simulation under the same conditions (Fig. 9). The results show that the two are similar in ice force variation trend and fluctuation amplitude, which indicates that the results of simulation program are consistent with the experimental data qualitatively.

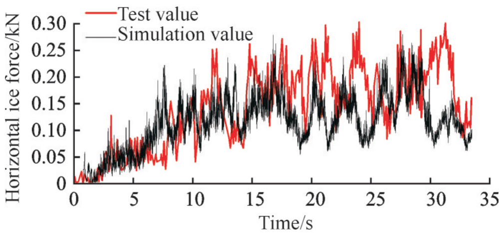

Fig.9 Comparison of ice force time traces between experiment and simulation

In terms of quantification, the simulation values of 10 working conditions, such as C_003, C_004, C_005, and C_006, are selected and compared with the corresponding experimental values. Since the maximum load and minimum load are instantaneous concepts, the interaction between sea ice and the structure is full of randomness, resulting in uncertainty of the timing and value of maximum and minimum values, thus losing its statistical significance. Mean load and peak load are statistical concepts, where peak load is defined as the sum of the mean value of ice–force time history and the standard deviations of 1.5 times the ice–force time history in the same time period in the stable stage. It can eliminate the slightly high data points generated by the vibration of the test model and comprehensively reflect the average maximum load in the interaction between the structure and ice load, which is the key data to be paid attention to in the study of ice load.

The simulation data are used as the x axis and the experimental data as the y axis. The data points are linearly fitted, and Fig. 10 is drawn (in the figure, R is the linear correlation coefficient). Through calculation and observation, it can be seen that the linear degree of horizontal mean load, peak load, vertical mean load, and peak load is relatively high, and the data points are distributed near the $y = x$ line. It can be considered that the numerical simulation has high accuracy. In general, the simulation program has certain accuracy, which can be further calculated and analyzed.

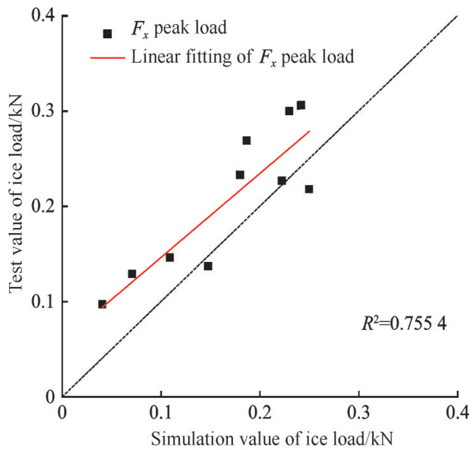

(a) Peak load of horizontal ice force

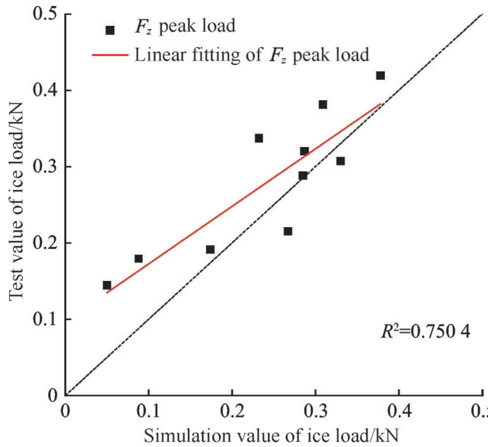

(b) Peak load of vertical ice force

Fig.10 Comparison of ice load between experiment and simulation

The study of ice load has been widely used in the ice–resistant safety performance of ships and marine structures. After consulting the ice–condition data in the polar region [10–11], we believe that all the sea ice acting on the external platform is flat ice, and the structure and sea–ice related parameters are determined as shown in Table 6.

We can obtain the time history data of horizontal and vertical ice forces by simulating the interaction between the nuclear power platform in the ice region and the flat ice with the thickness of 1 m and drift velocity of v = 0.2, 0.35, and 0.5 m/s. Figs. 11–12 take ice drift velocity of 0.5 m/s as an example to give the distribution of crushed ice and time history of ice

Table 6 Related parameters of sea ice and structure

Parameter	Value	Parameter	Value
Diameter at waterline D/m	93.36	Ice compression strength σ_c/MPa	1.5
Diameter at top surface D_t/m	77	Elastic modulus E/Gpa	1.0
Cone angle of platform α/(°)	60	Poisson ratio υ	0.3
Angle between crushed ice and horizontal plane θ/(°)	55	Porosity e	0.3
Friction angle of crushed ice φ/(°)	40	Cohesion c/ kPa	24
Ice-structure friction coefficient μ	0.3	Specific gravity of water γ	10 176.12
Ice-ice friction coefficient μ_i	0.1	Specific gravity of ice γ_i	9 045.44
Ice thickness h/m	1	Ice drift velocity v/(m·s^{-1})	0.2~0.5
Ice bending strength σ_f/MPa	1.0	Ice–structure contact width B/ m	5

load, respectively.

Since the initial position of the structure is not in contact with the ice field, the ice load is 0. With the interaction between the ice field and the platform, the ice force gradually increases. When the cut–in depth of the ice field exceeds the platform radius, the ice load tends to be stable, which can be regarded as a stable stage. At the later stage of the stability stage, a new peak may appear due to the accumulation of crushed ice until the end of the simulation. Under the three kinds of ice velocities, 250, 150, and 100 s are taken into the stable stage respectively, and the mean load and peak load of the horizontal and vertical ice forces are calculated, as shown in Fig. 13.

As can be seen from Fig. 13, with the increase in ice drift velocity, the ice load rises obviously. The reason is that the nuclear power platform is a large–scale structure. With the increase in ice drift velocity, the accumulation of crushed ice becomes more serious, resulting in the increase in total mass and impact force as well as the decrease in action time, which leads to the rise in sea ice force. The accumulation of crushed ice is shown in Fig. 14.

3.3 Combined effect of ice, wind, and current

We can obtain the time history of heave, roll, and pitch responses by applying ice forces of time histories obtained by numerical simulation to the environmental bearing platform (Fig. 15). Then we calculate by coupling the time history with wind and current loads. The wind load is taken as wind speed of level 6 and the wind direction is 90°. The selected flow velocity of the current load is consistent with the ice drift velocity and the flow direction is 0°. Under the driving of sea ice, wind, and current loads, as well as the constraints of connecting mechanism and mooring system, the nuclear power platform deviates from

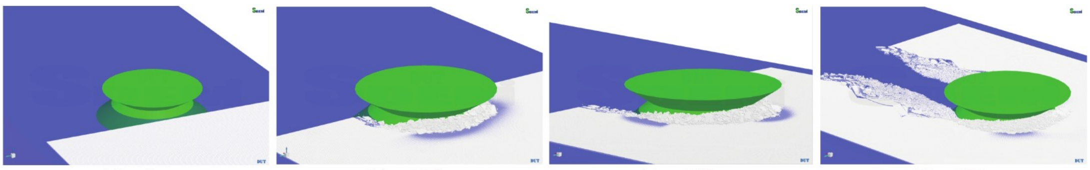

(a) t=0 s (b) t=100 s (c) t=200 s (d) t=700 s

Fig.11 Simulation of interaction between ice load and environmental bearing platform (ice drift velocity is 0.5 m/s)

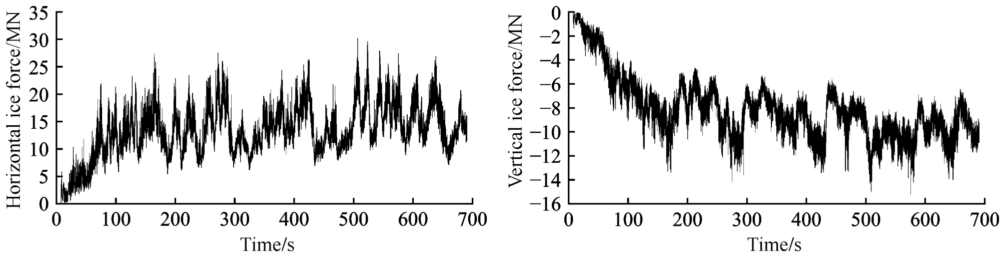

(a) Horizontal ice force (b) Vertical ice force

Fig.12 Time history of horizontal and vertical ice force (ice drift velocity is 0.5 m/s)

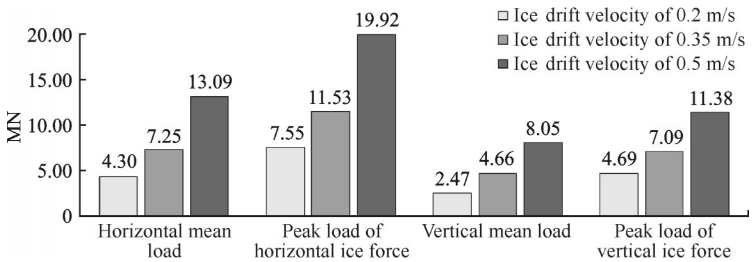

Fig.13 Effect of ice drift velocity on ice load

(a) Less accumulation of crushed ice at ice drift velocity of 0.2 m/s (b) Heavy accumulation of crushed ice drift at ice velocity of 0.5 m/s

Fig.14 Crushed ice accumulation

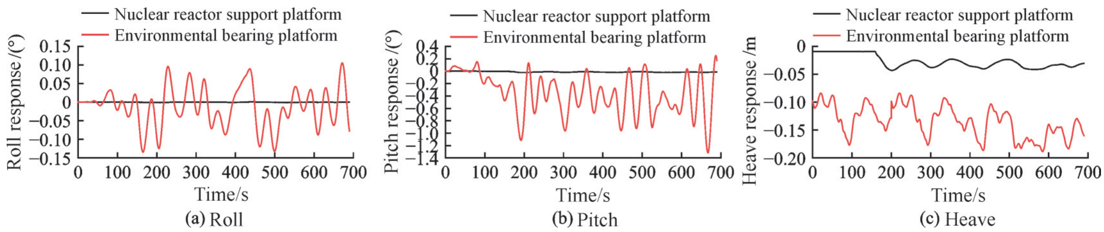

Fig. 15 Time history of motion response of nuclear power platform (ice drift velocity of 0.5 m/s)

Table 7 Maximum motion response for combined action of ice, wind, and current

Degree of freedom	Nuclear reactor support platform			Environmental bearing platform		
	v=0.2 m/s	v=0.35 m/s	v=0.5 m/s	v=0.2 m/s	v=0.35 m/s	v=0.5 m/s
Surge /m	1.392	1.525	2.480	1.651	1.670	3.070
Sway /m	1.282	1.355	1.685	1.334	1.405	1.766
Heave /m	0.004	0.007	0.017	0.057	0.078	0.131
Roll /(°)	0.001	0.001	0.002	0.138	0.126	0.170
Pitch /(°)	0.008	0.014	0.027	0.310	0.407	1.409
Yaw /(°)	0.002	0.016	0.019	0.008	0.011	0.053

the initial position to reach a new equilibrium position and finally continues to oscillate, obtaining the maximum motion response subjected to the combined effect of ice, wind, and current, as shown in Table 7.

From the calculation results, it can be seen that the environmental bearing platform has a small motion response under the combined effect of 1 m-thick flat ice, wind, and current loads, and has a good performance of ice resistance. The connecting mechanism can weaken the impact of the external platform on the internal platform and ensure the safety of the nuclear reactor. Under the combined effect of ice, wind, and current, the maximum acceleration of nuclear reactor is 0.000 7g, 0.000 9g, and 0.002 3g respectively, which meets the limitation requirements on acceleration of land-based nuclear reactor.

Nuclear reactors, which release a large amount of heat when they are working properly, need a steady stream of seawater to cool them down, so there is little chance that moon pools will freeze during an ice period. If the reactor is shut down, the moon pool could freeze. It is assumed that there is no relative velocity between the internal and external platforms due to icing, which leads to the failure of the damper, and then the ice load can restrict the relative movement in the horizontal plane of two platforms. In addition, because the external platform is designed as a vertebral structure with excellent ice resistance, its motion response amplitude under ice load is small, so there is no need to worry about the movement of the internal platform under this situation.

4 Conclusions

In this paper, the concept of a new separated ice region marine nuclear power platform is presented. The design of connecting mechanism of the platform is introduced, and the motion response of the platform under combined effect of wave, wind, and current with ice, wind, and current is analyzed. The spring damping force on the platform is calculated. Moreover, the damping coefficient of the connecting mechanism and characteristics of the spring stiffness coefficient are studied, and the optimal damping stiffness scheme is selected to limit the motions in the surge and sway degree-of-freedoms of the platform and to reduce vibration. The main conclusions are as follows:

1) In this paper, the concept of a new offshore nuclear power platform in the separated ice region is proposed, especially the spring-damped connecting mechanism, which has a good hydrodynamic performance and can resist the combined effect of the maximum tsunami wave height and level 17 super typhoon in the Fukushima nuclear leakage accident. Moreover, under the action of a 10 000-year return-time storm in the North Sea, the ratio of horizontal displacement to the water depth, heave and pitch responses and vertical acceleration of the platform supported by the nuclear reactor are all smaller than those of OFNP platform proposed by the research team of MIT.

2) The nuclear power platform has good ice resistance capability, and the environmental load bearing platform can resist the ice load well. The design of the connecting mechanism can well limit the surge and sway of the internal platform and play a role in reducing vibration. The external platform acts as a barrier to the marine dynamic environment, greatly improving the motion performance of the platform supporting the nuclear power plant and making its six-degrees-of-freedom motion response relatively small.

3) The design scheme of the pure mechanical connecting mechanism reduces the impact of the roll and pitch of the external environment bearing platform on the internal nuclear reactor support platform and effectively guarantees the safety of the nuclear reactor. This mechanism adopts the pure mechanical method, with good motion control, energy saving, environmental protection, and cost-effectiveness, which can provide technical reserve for related research.

References

[1] ZVEREV D L, FADEEV Y P, PAKHOMOV A N, et al. Nuclear power plants for the icebreaker fleet and power generation in the Arctic region: development experience and future prospects [J]. Atomic Energy, 2019, 125 (6): 359-364.

[2] CHU S, MAJUMDAR A. Opportunities and challenges for a sustainable energy future [J]. Nature, 2012, 488 (7411): 294-303.

[3] LEE K H, KIM M G, LEE J I, et al. Recent advances in ocean nuclear power plants [J]. Energies, 2015, 8 (10): 11470-11492.

[4] BUONGIORNO J, JUREWICZ J, GOLAY M, et al.The offshore floating nuclear plant concept [J]. Nuclear Technology, 2016, 194 (1): 1-14.

[5] ZHANG Y L, BUONGIORNO J, GOLAY M, et al.Safety analysis of a 300-MW (electric) offshore floating nuclear power plant in marine environment [J]. Nuclear Technology, 2018, 203 (2): 129-145.

[6] Dalian University of Technology. Nuclear power platform applicable to ice zone: CN, 201710906994.7 [P]. 2018-02-09 (in Chinese).

[7] JI S Y, WANG S L. A coupled discrete-finite element method for the ice-induced vibrations of a conical jacket platform with a GPU-based parallel algorithm [J]. International Journal of Computational Methods, 2020, 17 (4): 1850147.

[8] XIE Q, CHEN H L, ZHANG J F. Research progress of anti-icing/deicing technologies for polar ships and offshore platforms [J]. Chinese Journal of Ship Research, 2017, 12 (1): 45-53 (in Chinese).

[9] IRANI M B, TIMCO G W. Ice loading on a multifaceted conical structure [C] //The Third International Offshore and Polar Engineering Conference. Singapore: International Society of Offshore and Polar Engineers, 1993: 313-321.

[10] HAN H W, LI Z J, HUANG W F, et al. The uniaxial compressive strength of the Arctic summer sea ice [J]. Acta Oceanologica Sinica, 2015, 34 (1): 129-136.

[11] KE C Q, WANG M M. Seasonal and interannual variation of thinkness and volume of the Arctic sea ice based on Cryo Sat-2 during 2010-2017 [J]. Acta Oceanologica Sinica, 2018, 40 (11): 1-13 (in Chinese).

[*Continued on page* 92]

不同截面形状下弹性支撑多跨梁振动特性分析

鲍四元*, 周静
苏州科技大学 土木工程学院,江苏 苏州 215011

摘　要:[**目的**]为克服边界及弹性横向支撑对连续多跨梁振动特性研究的束缚,基于欧拉梁理论,建立一种多跨梁自由振动的分析模型。[**方法**]首先,构造新型改进傅里叶级数形式,用以表示多跨梁在整段上的横向位移函数;其次,将位移函数的级数表达式代入拉格朗日函数中,结合瑞利—里兹法,将自由振动问题变为标准矩阵特征值形式,以求解带有弹性支撑的多跨梁固有频率。[**结果**]通过在算例部分改变弹性支撑处的横向弹簧刚度值,即可获得中间含任意弹性支撑多跨梁的振动特性,所得结果与已有文献结果的比较充分验证了所提方法可行且正确。[**结论**]基于改进傅里叶级数法(IFSM),多跨梁振动特性的数值模拟可为多跨梁动态性能提供有效的前期预测手段。

关键词:多跨梁; 弹性支撑; 固有频率; 改进傅里叶级数方法

[*Continued from page* 83]

核电平台连接机构设计与运动响应分析

李想, 李红霞*, 黄一
大连理工大学 船舶工程学院,辽宁 大连 116024

摘　要:[**目的**]为满足深海冰区海洋核反应堆安全工作的要求,设计冰区核电平台与弹簧阻尼连接机构。[**方法**]利用三维势流理论及刚体动力学理论建立平台与连接机构的仿真模型。计算平台所受弹簧阻尼力,研究连接机构刚度、阻尼系数特性,选择最佳方案。应用离散元法进行冰载荷数值模拟,通过计算试验椎体所受冰载荷,验证该方法的准确性。研究浪、风、流或海冰、风、流环境载荷联合作用下平台的运动响应。[**结果**]结果显示,平台系泊于深海冰区可远离海啸的影响,环境承载平台能较好抵抗冰载荷;在连接机构与系泊系统的作用下,核堆支撑平台可抵御福岛核泄漏事故最大海啸波高与17级超强台风的联合作用;在北海万年一遇风暴作用下,核堆支撑平台的水平位移与水深之比、垂荡与纵摇响应及垂向加速度均小于海上浮动核电平台(OFNP)。[**结论**]核电平台与连接机构的设计可保证应用于深海冰区的核堆的安全稳定。

关键词:核电平台; 连接机构; 冰载荷; 减振; 运动响应; 系泊